CSCanada
Advances in Petroleum Exploration and Development
Vol. 11, No. 2, 2016, pp. 64-69
DOI:10.3968/8594

ISSN 1925-542X [Print]
ISSN 1925-5438 [Online]
www.cscanada.net
www.cscanada.org

Modelling on the Evolution of Corrosion Pit During Stress Corrosion

LI Junquan[a],*

[a] Huangling Exploration and Development Project Headquarter of Yangchang Oil Field CO., LTD, Huangling, China.
*Corresponding author.

Received 28 May 2016; accepted 23 June 2016
Published online 26 June 2016

Abstract
Corrosion pit always changes its shape and size during stress corrosion. The actual morphology of pit is the outcome of the interaction between the variation in the elastic energy induced by far-field stress, surface energy of pit surface and electrochemical energy stored in the stressed solid. Based on the semi-ellipsoidal pit assumption, an explicit expression that controls the evolving morphology of pit is introduced, from which the effects of specific parameters to pit morphology are studied. According to the stress intensity factor criterion for pit transition to crack, the crack nucleation life is also discussed.

Key words: Aluminium; Modelling studies; Stress corrosion; The crack nucleation life

Li, J. Q. (2016). Modelling on the evolution of corrosion pit during stress corrosion. *Advances in Petroleum Exploration and Development*, *11*(2), 64-69. Available from: URL: http://www.cscanada.net/index.php/aped/article/view/8594
DOI: http://dx.doi.org/10.3968/8594

INTRODUCTION
Stress corrosion is a typical physical-electrochemical process that leads to materials degradation and failure of engineering structures. Stress promotes the formation of corrosion pits and transition from pits to cracks of material in aggressive environment and shortens the service life of structures[1-3]. Pits almost always initiate at some chemical or physical heterogeneity on the surface. Materials such as high-strength aluminum alloys contain numerous constituent particles, which play an important role in corrosion pit formation[4-5]. With pitting corrosion degradation being recognized as a potential cause for structural failures, the need for predictive methodologies and models of corrosion cannot be overlooked. The pit morphology was indicated mainly decided by electrochemical processes in metal/electrolyte interface and potential distribution inside the cavities[6-9]. And the pit morphology appears in hemispherical shape at early stage of growth when developed tends to transit from hemispherical to cylindrical or to dish shape[10]. To idealize the growing model of pit, a semi-sphere pit model growing at equal rate at all direction was assumed by Godard[11], and this model was generalized as semi-ellipsoidal, and there different approaches were proposed to depict the evolving morphology of pits[12-13]. But it is not clear what sort of conditions must be fulfilled to obtain pits in a particular shape.

As reviewed above, the models to predict the pit evolution during stress corrosion are available. But the predictive results were difficult to get good agreement with the experimental appearance in Ref. In this paper, we attempt to establish the pit evolving model from energy approach. Stress corrosion is an irreversible thermodynamics process, as well as the pit morphology is controlled by the variation of thermodynamic potential. A suitable thermodynamic potential of the material model with an evolving single pit is established, from which some dimensionless parameters that control the pit evolution is introduced. Then, an explicit expression is derived for the prediction of evolving morphology of corrosion pit, from which the crack nucleation life of the stress corrosion is estimated.

1. THEORETICAL METHOD

1.1 Model of the Evolving Pit
Figure 1 shows the three-dimensional model of a corrosion pit in the semi-infinite elastic solid. Based on

the symmetry of the problem, the corrosion pit can be idealized as a semi ellipsoid, and the cross-section of the pit in *xy* plane maintains semicircle Let *a*, *b* and *c* be semi axes in *x*, *y* and *z* direction, respectively.

$$a = b = r\sqrt{\frac{1+m}{1-m}}, \quad c = r\frac{1-m}{1+m}. \tag{1}$$

Where, *m* is the shape parameter of semi-ellipsoidal pit, ranging -1<*m*<1, *r* is the radius of the hemisphere having the same volume with the semi-ellipsoidal pit. The hemisphere corresponds to *m*=0, the x-y direction crack to *m*→+1, and the thin-strip vertical crack to *m*→-1.

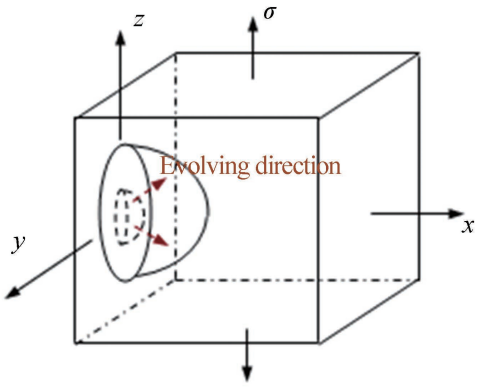

Figure 1
The Semi-Ellipsoidal Pit in Semi-Infinite Elastic Solid During Stress Corrosion

The symmetry of the above model always meets during the stress corrosion, so the actual evolving morphology of pit can be indicated as the sequences of semi ellipsoid, with its *x*-*z* section shown in Figure 2. According to Equation (1), the morphology at any time can be clearly characterized by pit depth *a* and shape parameter *m*, that is

$$\Psi = \Psi(a, m). \tag{2}$$

Where, Ψ is the variable to characterize the pit morphology during evolving process.

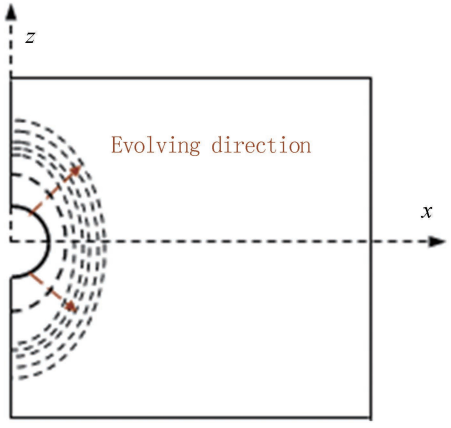

Figure 2
The *x*-*z* Cross Section of Evolving Semi-Ellipsoidal Pit in Semi-Infinite Elastic Solid

1.2 The Thermodynamic Potential of Elastic Solid With an Evolving Corrosion Pit

The thermodynamic potential of elastic solid consists of elastic energy, surface energy and electrochemical energy. When pit evolves constantly under the interaction of corrosion environment and cycle stress, the pit varies shape and size, the solid varies its elastic energy and surface energy, and anodic dissolution of pit releases electrochemical energy. So the thermodynamic potential can be seen as a functional of pit shape, pit volume, the applied cyclic load. The thermodynamic potential energy of the elastic solid with an evolving pit can be expressed as

$$\Phi = U_E + U_C + U_S. \tag{3}$$

Where, Φ is thermodynamic potential of elastic solid, U_E is strain energy, U_C is the released electrochemical energy during the corrosion process, and U_S is surface energy.

As pit varying its morphology during corrosion fatigue, the anode dissolution releases electrochemical energy, the elastic solid changes its elastic energy, and the variation of pit surface changes surface energy.

The semi-infinite elastic solid containing a semi-ellipsoidal pit subjected to remote cyclic stress stores infinite amount of strain energy. Yet, the energy difference between the solid containing a semi-ellipsoidal pit to the solid without pit subjected to the same stresses can be computed by Eshelby inclusion theory[14-16].

$$\Delta U_E = \frac{2\pi a^3 \sigma^2}{3E}\left(\frac{1-m}{1+m}\right)^{3/2} B. \tag{4}$$

Where, *E* is the young modulus, σ is the remote stress, and *B* is the dimensionless coefficient, as a function of the shape parameter *m*, and the Poisson's ratio *v*, specifically expressed as

$$B = \frac{1 - S_{11} - S_{12} - 2\nu S_{31}}{(1 - S_{33})(1 - S_{11} - S_{12}) - 2S_{31}S_{13}}. \tag{5}$$

Where, S_{ij} can be found in Eshelby.

When the initial pit grows to a random state, with pit depth varying from a_0 to *a*, the elastic energy differs by

$$\Delta U_E = -\frac{2\pi\sigma^2}{3E}\left(\left(\frac{1-m}{1+m}\right)^{3/2} a^3 B - \left(\frac{1-m_0}{1+m_0}\right)^{3/2} a_0^3 B_0\right). \tag{6}$$

Where, a_0, B_0 is *a* and *B* for the initial pit.

The surface area of pit changes during evolution, leading to the variation of surface energy. Introducing the dimensionless coefficient *A*,

$$A = \zeta^2/2 + \ln\left(\left(\zeta^6 - 1\right)^{1/2} + \zeta^3\right) / \left(2\zeta\left(\zeta^6 - 1\right)^{1/2}\right). \tag{7}$$

Where, $\zeta = \left[(1+m)/(1-m)\right]^{1/2}$.

The surface area of pit is written as

$$S = 2\pi r^2 A. \tag{8}$$

Then the variation of surface energy is

$$\Delta U_S = 2\pi\gamma_S\left(\left(\frac{1-m}{1+m}\right)^2 a^2 A - \left(\frac{1-m_0}{1+m_0}\right)^2 a_0^2 A_0\right). \tag{9}$$

Where, γ_s is the surface energy per area on the pit surface, A_0 is A for the initial pit.

The elastic solid releases electrochemical energy by anodic dissolution when pit evolves. According to the electrochemical mechanism of corrosion, the released electrochemical energy during pit evolution equals to the done work of the dissolved metal's power in the electric field. Let ρ be the density, M be the molecular quality, and n be valence, when the pit evolves to the critical state from the initial state, the power of dissolved anode metal is

$$\Delta Q = \frac{2\pi\rho}{3M}\left(\left(\frac{1-m}{1+m}\right)^{3/2} a^3 - \left(\frac{1-m_0}{1+m_0}\right)^{3/2} a_0^3\right) nF . \quad (10)$$

Where, $F = Ne$ is the Faraday constant, and $N = 6.023\times10^{23}$ is atoms number of per Moore metal.

According to thermodynamics principle, the anodic potential of the corrosion battery can be expressed as

$$E_0 = E^{\oplus} + \frac{RT}{nF}\ln a_M^{n+} . \quad (11)$$

Where, $E^{\oplus}$ is metal's standard electrode potential, R is universal gas constant, T is absolute temperature, and a_M^{n+} is activity of metal ion.

Assuming the anodic potential of the corrosion battery remains unchanged during pit evolution, the variation of electrochemical energy is

$$\Delta U_C = -E_0 \times \Delta Q = -\left(E^{\oplus} + \frac{RT}{nF}\ln a_M^{n+}\right)\times\frac{2\pi\rho}{3M}\left(\left(\frac{1-m}{1+m}\right)^{3/2} a^3 - \left(\frac{1-m_0}{1+m_0}\right)^{3/2} a_0^3\right) nF . \quad (12)$$

So the variation of thermodynamic potential $\Delta\Phi$ can be rewritten as

$$\Delta\Phi = -\frac{2\pi\sigma^2}{3E}\left(\left(\frac{1-m}{1+m}\right)^{3/2} a^3 B - \left(\frac{1-m_0}{1+m_0}\right)^{3/2} a_0^3 B_0\right) + 2\pi\gamma_S\left(\left(\frac{1-m}{1+m}\right)a^2 A - \left(\frac{1-m_0}{1+m_0}\right)a_0^2 A_0\right) - E_0\times\frac{2\pi\rho nF}{3M}\left(\left(\frac{1-m}{1+m}\right)^{3/2} a^3 - \left(\frac{1-m_0}{1+m_0}\right)^{3/2} a_0^3\right) \quad (13)$$

1.3 The Evolving Morphology of Corrosion Pit

According to the second law of thermodynamics, the system energy dissipation rate is positive during the evolution of pit, consequently the thermodynamic potential decreases continuously. But among all possible morphologies of pit, the actual pit morphology minimizes Φ.

Expand Equation (13) in powers of a and m,

$$\Delta\Phi = -\Lambda\left[a^3\left(1-2.625m+1.995m^2-3.15m^3+\cdots\right) - \left(\frac{1-m_0}{1+m_0}\right)^{3/2} a_0^3 B_0\right] + \Gamma\left(a^3\left(1-3m+4.5m^2-6m^3\right) - \left(\frac{1-m_0}{1+m_0}\right)^{3/2} a_0^3\right) + 2\pi\gamma_S\left[a^2\left(1-2m+3.6m^2-4.44m^3+\cdots\right) - \left(\frac{1-m_0}{1+m_0}\right)a_0^2 A_0\right] . \quad (14)$$

Here, only three leading terms are retained for small m. Obviously, the th.eoretical pit shape requires $d\Phi/dm=0$, that is

$$\left(9.45\Lambda a^3 - 18\Gamma a^3 - 26.72\pi\gamma_S a^2\right)m^2 + \left(14.4\pi\gamma_S a^2 + 9\Gamma a^3 - 3.99\Lambda a^3\right)m + \left(2.625\Lambda a^3 - 3\Gamma a^3 - 4\pi\gamma_S a^2\right) = 0 . \quad (15)$$

Where, $\Lambda = \frac{2\pi\sigma^2}{3E}$, $\Gamma = -\left(E^{\oplus} + \frac{RT}{nF}\ln a_M^{n+}\right)\times\frac{\pi\rho nF}{2M}$.

The actual pit shape m is

$$m = -\left(14.4\pi\gamma_S + 9\Gamma a - 3.99\Lambda a\right) + \omega^{1/2}\Big/2\left(9.45\Lambda a - 18\Gamma a - 26.72\pi\gamma_S\right) , \quad (16)$$

where, $\omega = \left(27\Gamma^2 + 39.69\Gamma\Lambda - 8.89\Lambda^2\right)a^2 + \left(50.48\pi\gamma_S\Lambda - 22.56\pi\gamma_S\Gamma\right)a + 100.48\pi^2\gamma_S^2$.

The shape parameter varies with the increase of pit depth according to Equation (16). If the solution of Equation (16) is within the range $-1 < m < 1$, the actual pit evolves at a particular morphology, otherwise the pit evolution is extremely unstable and collapses to the crack quickly.

2. STRESS CORROSION CRACK NUCLEATION

Stress corrosion cracks nucleates and propagates from corrosion pits, which had been confirmed by a lot of studies[17-18]. Corrosion pit may transit to crack when evolving to a certain stage, so corrosion pit can be seen as a precursor to stress corrosion cracking. But few studies have involved the model for corrosion pit transition to stress corrosion cracking. Learning from the transition model for pitting to corrosion fatigue crack nucleation[19-22], we can set up the criterion of corrosion pit transiting to stress corrosion crack .The semi-infinite elastic solid containing a semi-ellipsoidal surface pit is equivalent to an infinite plate consisting of semicircular surface flaws in 2-D, shown in Figure 3. When the maximum stress intensity factor of such a plate reaches to the stress corrosion threshold stress intensity K_{ISCC}, the corrosion pit begins to convert to stress corrosion crack, that is

$$K_{max} \geq K_{Iscc} \quad \text{and} \quad \sigma \leq \sigma_{SCC}. \tag{17}$$

Where, $K_{max} = \frac{1.12k_t\sigma\sqrt{\pi a}}{\Omega}$, $\Omega = \int_0^{\pi/2}\left[\sin^2\theta + (c/a)^2\cos^2\theta\right]^{1/2} d\theta$, k_t is stress concentration factor, σ_{SCC} is the stress corrosion threshold stress.

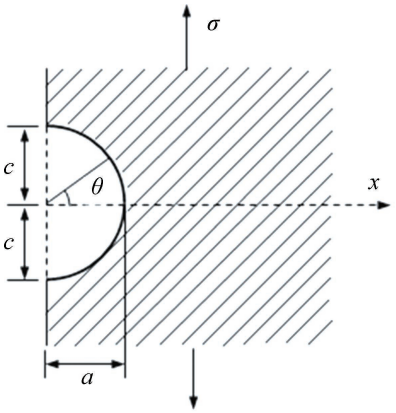

Figure 3
The Equivalent Semi-Elliptic Surface Crack Modeled From Corrosion Pit Causing Stress Corrosion Crack Nucleation

Thus, the critical pit depth a_{cr} when corrosion pit transition to crack is found to be

$$a_{cr} = \frac{1}{\pi}\left(\frac{K_{Iscc}\Omega_{cr}}{1.12k_t\sigma}\right)^2. \tag{18}$$

Where, Ω_{cr} is Ω at critical pit size.

Substituted Equation (16) into Equation (18) so the critical pit depth a_{cr} and shape parameter m_{cr} can be obtained and the critical pit morphology is determined. Applying the Faraday's law[23], the stress corrosion crack nucleation life can be determined.

$$\frac{dV}{dt} = \frac{MI_{P0}}{nF\rho}\exp\left(-\frac{\Delta H}{RT}\right). \tag{19}$$

Where, V is the volume of pit, I_{p0} is the pitting current coefficient, depending on the clustered particles, and ΔH is the activation energy.

Integrating Equation (19), we have

$$\Delta V = \frac{2\pi}{3}\left(\left(\frac{1-m_{cr}}{1+m_{cr}}\right)^{3/2} a_{cr}^2 - \left(\frac{1-m_0}{1+m_0}\right)^{3/2} a_0^2\right) = \frac{MI_{P0}}{nF\rho}\exp\left(-\frac{\Delta H}{RT}\right)t. \tag{20}$$

Where, a_0, m_0 are a and m when pit initiates.

Thus the stress corrosion crack nucleation life is written as

$$t_{p\text{-}c} = \frac{2\pi nF\rho}{3MI_{P0}}\left(\left(\frac{1-m_{cr}}{1+m_{cr}}\right)^{3/2} a_{cr}^3 - \left(\frac{1-m_0}{1+m_0}\right)^{3/2} a_0^3\right)\exp\left(\frac{\Delta H}{RT}\right). \tag{21}$$

3. NUMERICAL CALCULATION AND DISCUSSION

From Equation (16), it can be seen that pit shape parameter varying with pit depth is controlled by the interaction between remote stress σ, surface energy γ_s and Γ relating to electrochemical energy. In this section we examine the pit evolution from an initial pit of ideal three-dimensional solid of aluminum alloy. The relative parameters are taken from the literature[24-25]: $M = 27\times10^{-3}$ kg/mol, $n = 3$, $F = 96{,}485$ C/mol, $\rho = 2{,}700$ kg/m^3 $R = 8.314$ J/molk, $T = 293$ K, $E = 7.2\times10^{10}$ N/m^2, $I_{P0} = 3.52\times10^{-2}$ C/s, $v = 1/3$, $\Delta H = 40$ KJ/mol, $\gamma_S = 2.4$J/m^2, $a_0 = 1\times10^{-3}$mm, $a_M^{n+} = 0.00089$ mol/L, $E^{\oplus} = -1.662$ V, $\sigma = 100$ MPa, $K_{Iscc} = 8.3$ MPa$\sqrt{\text{m}}$, $k_t = 2.8$, $\sigma_{SCC} = 70$ MPa.

The influences of σ, γ_s and Γ on shape parameter m varying with pit depth a are respectively shown in Figures 4-6. The morphology of the initial pit approximately is a hemisphere that when developed turns into a semi-ellipsoidal with shape parameter gradually close to a stable value.

The influence of σ to shape parameter is more obvious and the pit is more likely changing its shape and stabilizing to the determinate value at higher σ level. The effect of surface causes the pit to maintain the morphology which contains minimum surface energy. So the pit tends to maintain the shape which contains as γ_s increases. So the pit inclines to maintain the initial shape of hemisphere, and the shape parameter of pit changes difficultly with the increase of a at higher γ_s level. The influence of electrochemical energy on shape parameter m is enhanced with the increase of Γ, and Pitt shape parameter varies more easily with increase of a.

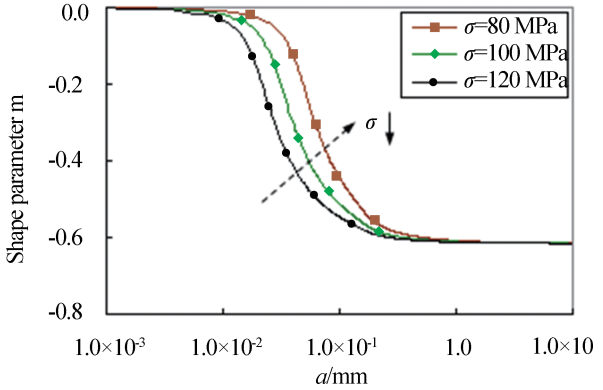

Figure 4
The Shape Parameter *m* as a Function of *a* at Different *σ* Levels

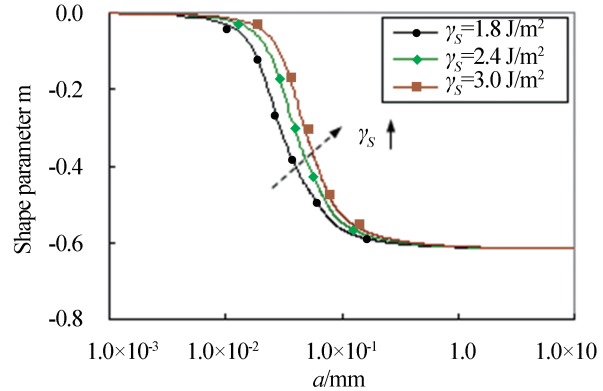

Figure5
The Influence of *a* on Shape Parameter *m* at Different γ_s Levels

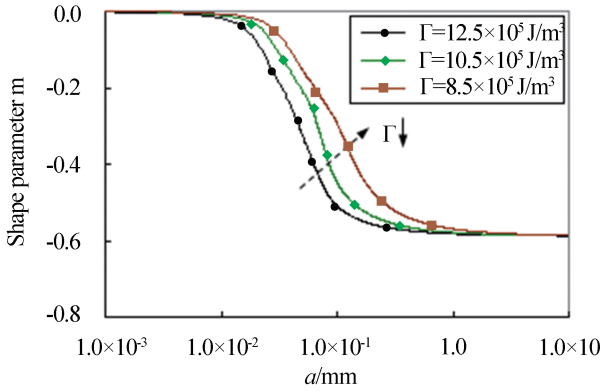

Figure 6
The Shape Parameter *m* Varies With *a* at Different Γ Levels

The influence of remote stress on crack nucleation life of stress corrosion is depicted in Figure 7. It can be seen that the crack nucleation life increases with the decrease of remote stress. When the remote stress declines below to the stress corrosion threshold stress, the stress corrosion has infinite life and Equation (21) is no longer applicable.

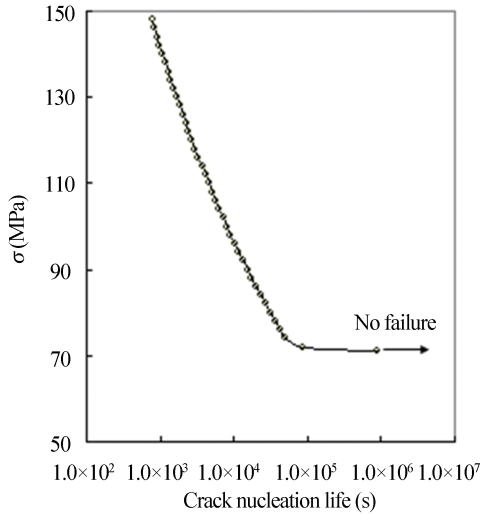

Figure7
Variation in Crack Nucleation Life With Remote Stress *σ*

CONCLUSION

A new approach is proposed to predict the pit evolving morphology during stress corrosion. The corrosion pit appears approximately as a hemisphere in its early stage of growth, and when developed transits from semicircle to ellipsoid with shape parameter gradually close to a stable value. The elastic energy induced by far-field stress, surface energy of pit surface and electrochemical energy stored in the stressed solid all have significant effects on the pit evolving morphology.

Connected with pit evolving equation, crack nucleation life of stress corrosion is evaluated by Farady law. Remote stress has significant effect on the crack initiation life. The higher stress amplitude, the shorter crack initiation life is. When the remote stress declines below to the stress corrosion threshold stress, stress corrosion has infinite life for crack nucleation.

REFERENCES

[1] Ruiz, J., & Elices, M. (1997). The role of environmental exposure in the fatigue behaviour of an aluminium alloy. *Corros. Sci.*, *39*(12), 2117-2141.

[2] Maeng, W. Y., Kang, Y. H., Nam, T. W., Ohashi, S., & Ishihara, T. (1999). Synergistic interaction of fatigue and stress corrosion crack growth behaviour in alloy 600 in high temperature and high pressure water. *J. Nucl. Mater.*, (275), 194-200.

[3] Congleton, J., Charles, E. A., & Sui, G. (2001). Review on effect of cyclic loading on environmental assisted cracking of alloy 600 in typical nuclear coolant waters. *Corros. Sci.*, *43*, 2265-2279.

[4] Wang, Q. Y., Pidaparti, R. M., & Palakal, M. J. (2001). Comparative study of corrosion-fatigue in aircraft materials. *AIAA Journal*, *39*(2), 325-330.

[5] Liao, C. M., & Wei, R. P. (1999). Galvanic coupling of model alloys to aluminum–a foundation for understanding particle–induced pitting in aluminum alloys. *Electrochim. Acta*, *45*, 881-888.

[6] Wei, R. P. (2001). A model for particle-induced pit growth in aluminum alloys. *Scripta Mater*, *44*, 2647-2652.

[7] Perkins, K. M., & Bache, M. R. (2005). Corrosion fatigue of a 12% Cr low pressure turbine blade steel in simulated service environments. *Int. J. Fatigue*, *27*, 1499-1508.

[8] Ghali, E., & Dietzel, W. (2004). Testing of general and localized corrosion of magnesium alloys: A critical review. *JMEPEG*, *13*, 7-23.

[9] Codaro, E. N., Nakazato, R. Z., Horovistiz, A. L., Ribeiro, L. M. F., Ribeiro, R. B., & Hein, L. R. O. (2002). An image processing method for morphological characterization and pitting corrosion evaluation. *Mater. Sci. Engng. A*., (334), 298-306.

[10] Ernst, P., Laycock, N. J., Moayed, M. H., & Newman, R. C. (1997). The mechanism of lacy cover formation in pitting. *Corros. Sci.*, *39*(6), 1133-1136.

[11] Godard, H. P. (1960). Corrosion behavior of aluminum in natural waters. *Can. J. Chem. Eng.*, *38*, 167-173.

[12] Harlow, D. G., & Wei, R. P. (1994). Probability approach for prediction of corrosion and corrosion fatigue life. *AIAA J.*, *32*, 2073-2082.

[13] Harlow, D. G., & Wei, R. P. (1998). A probability model for the growth of corrosion pits in aluminum alloys induced by constituent particles. *Eng. Fract. Mech.*, *59*, 305-325.

[14] Eshelby, J. D. (1957). The determination of the elastic field of an ellipsoidal inclusion, and related problems. *Proceedings of the Royal Society of London, Series A, Mathematical and Physical Sciences*, (241), 376-396.

[15] Wang, H., & Li, Z. H. (2004). Stability and shrinkage of a cavity in stressed grain. *Journal of Applied Physics*, *95*(11), 6025-6031.

[16] Wang, H., & Li, Z. H. (2004). The three-dimensional analysis for diffusive shrinkage of a grain-boundary void in stressed solid. *Journal of Materials Science*, *39*, 3425-3432.

[17] Kondo, Y. (1987). Prediction method of corrosion fatigue crack initiation life based on corrosion pit growth mechanism. *Trans. Japan Soc. Mech. Eng.* (*Ser. A*), *53*(495), 1983-1987.

[18] Chen, G. S., Wan, K. C., Gao, M., Harlow, D. G., & Wei, R. P. (1996). Transition from pitting to fatigue crack growth-modeling of corrosion fatigue crack nucleation in a 2024-T3 aluminum alloy. *Materials Science and Engineering A*, (219), 126-132.

[19] Turnbull, A., McCartney, L. N., & Zhou, S. (2006). Modelling of the evolution of stress corrosion cracks from corrosion pits. *Scripta Materialia*, *54*, 575-578.

[20] Turnbull, A., McCartney, L. N., & Zhou, S. (2006). A model to predict the evolution of pitting corrosion and the pit-to-crack transition incorporating statistically distributed input parameters. *Corrosion Science*, *48*, 2084-2105.

[21] Turnbull, A., Horner, D. A., & Connolly, B. J. (2009). Challenges in modelling the evolution of stress corrosion cracks from pits. *Engineering Fracture Mechanics*, *76*, 633-640.

[22] Horner, D. A., Connolly, B. J., Zhou, S., Crocker, L., & Turnbull, A. (2011). Novel images of the evolution of stress corrosion cracks from corrosion pits. *Corrosion Science*, *53*, 3466-3485.

[23] Rajasankar, J., & Iyer, N. R. (2006). A probability-based model for growth of corrosion pits in aluminum alloys. *Engineering Fracture Mechanics*, *73*, 553-570.

[24] Sriraman, M. R., & Pidaparti, R. M. (2010). Crack initiation life of materials under combined pitting corrosion and cyclic loading. *Journal of Materials Engineering and Performance*, *19*(1), 7-12.

[25] Harlow, D. G., & Wei, R. P. (2001). Probability modelling and statistical analysis of damage in the lower wing skins of two retired B-707aircraft. Fatigue Fract. *Eng. Mater. Struct.*, *24*, 523-535.

